Optimized Allocation of Loads in MMC-based Electric Vehicle Charging Infrastructure

Erdem Gümrükcü*, Ferdinanda Ponci*, Antonello Monti*, Giuseppe Guidi†, Salvatore D'Arco†, Jon Are Suul,†‡

*Institute for Automation of Complex Power Systems
E.ON ERC - RWTH Aachen University
Mathieustrasse 10, 52074 Aachen, Germany
erdem.guemruekcue@eonerc.rwth-aachen.de
fponci@eonerc.rwth-aachen.de
amonti@eonerc.rwth-aachen.de

†SINTEF Energy Research
7465 Trondheim, Norway
giuseppe.guidi@sintef.no
salvatore.darco@sintef.no

‡Department of Eng. Cybernetics
NTNU
77495 Trondheim, Norway
jon.are.suul@ntnu.no

***Abstract*—Utilization of the modular multilevel converter (MMC) topology can enable transformer-less interfacing between electric vehicle (EV) charging infrastructure and the power distribution grid. Such configurations are claimed to significantly reduce the system costs, space requirements and complexity for high-power charging facilities. On the other hand, ensuring the correct operation of such system is challenging under unevenly distributed loads in the MMC arms. Proper selection of the charging points to allocate the EVs can limit the loading unbalances between the arms and phases of the MMC system. This paper presents two load allocation strategies. The first strategy takes only the present loading into account, while the second one optimizes the decision according to the individual energy demands of the EVs over time. Simulations demonstrated that the optimized strategy minimizes loading unbalances between the MMC phases and arms during the charging operations. Furthermore, it can contribute to larger demand fulfillment.**

***Index Terms*—Charging infrastructure, electric vehicle, energy management, modular multilevel converter, optimization**

I. Introduction

In many countries, public authorities have set specific goals for electrification of the transportation sector and established incentives to promote electromobility. European governments aim to attract their citizens with reduced value-added-tax (VAT), registration fees and vehicle ownership tax [1]. Similarly in Japan zero emission cars are exempt from acquisition and tonnage taxes [2]. Norway implemented an incentive policy that enables free-of-charge parking in public parks (until 2017), opens bus lanes to EV use, and removes VAT and import taxes [3]. Numerous car manufacturers all around the world have been following the electrification trend and are investing in EV technologies in order to stay competitive in the future mobility market. As result of these parallel progresses the share of hybrid, plug-in hybrid and full electric cars have started to become significant in the traffic. It is anticipated that the number of EVs on the road will soon be significant [4].

Charging infrastructure is expected to become the backbone of the electromobility. Parking lots of commercial and public entities such as shopping malls, airports, event halls etc. will potentially accommodate a large number of charging nodes. Several works in the literature investigated large-scale EV charging applications considering various aspects such as demand response management [5], charging profile optimization [6], and network reinforcement requirements due the harmonic emissions [7]. On the other hand, the literature lacks studies that investigate the most suitable topology.

A charging facility that is capable of simultaneously hosting hundreds of EVs would require power installations in the multi-megawatt range [8]. This implies direct connection to the medium voltage distribution grid through dedicated distribution transformers with very large power rating, and potentially with several transformers for the same charging infrastructure. The level of power and complexity translates in large space coverage and high installation and operating costs; [9] estimates the installation costs for such scale up to several million euros. Consequently, technologies that could possibly reduce the infrastructure costs will be very valuable. Furthermore, the space constraints of densely populated areas will increase the importance of the compact solutions.

An EV charging configuration based on a modular multilevel converter (MMC) topology with wireless power transfer from the individual MMC cells is proposed in [10]. This configuration aims to reduce the overall system costs and size by transformer-less grid interfacing and lighter cabling. The considered application can present relatively large unbalances between MMC phases and arms due to different arrival/departure times and diverse individual demands of the EVs. Internal power flow in the charging system must be controlled in order for the MMC system to interface with the power grid as a 3-phase balanced entity despite the unbalanced distribution of the load. The previous works in this area focus on controlling the given unbalanced loading conditions [10], [11]. However, the ability of the MMC to cope with unbalanced loading would be limited by the switching devices and cables, and high unbalance can also generate additional losses. In case that the unbalance is beyond the controllable

978-1-7281-6350-5/20/$31.00 ©2020 IEEE

limits, active intervention such as suspension or reduction of the charging power would be needed. In certain scenarios, such interventions would result in low final SOC or longer charging duration, which are major concerns for EV users. Suitable operational strategies must be established in order to exploit the control capabilities that maximize the demand fulfillment.

A relevant control feature in a large charging facility is the ability to allocate the cars to specific chargers upon their arrivals. With a proper allocation strategy, the operator can limit the future unbalances in the system rather than only reacting to them. This paper addresses the problem of EV allocation in an MMC-based charging infrastructure, which is so far lacking in the scientific literature. Although the proposed strategies were designed considering the unique constraints of the MMC-based charging topology, it is possible to extend them for the use in other EV charging applications in which limiting the load on subsections of the system is necessary due to the undersized transformer, cables or, converter capacity with respect to the installed power of the chargers. Another relevant application could be the routing service for reserving charging spots in a multi-charging station scenario.

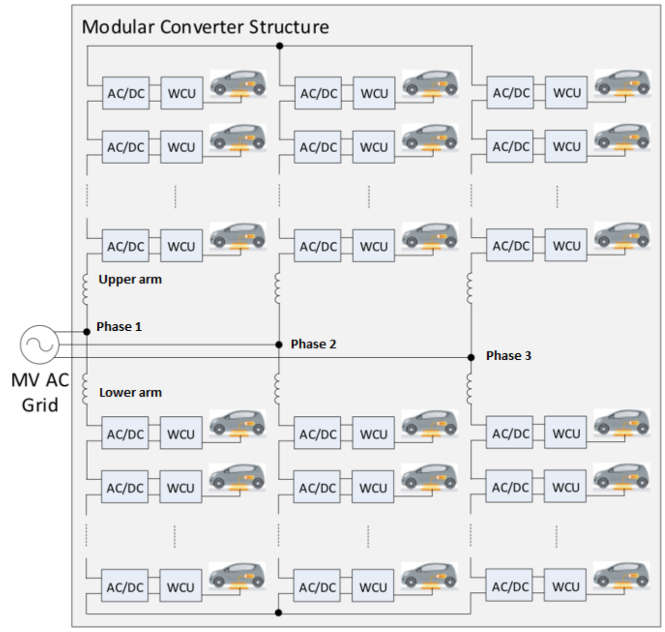

Fig. 1. Proposed connection layout of large charging infrastructure for wireless EV charging with MMC-based grid interface [10]

II. MMC-BASED CHARGING INFRASTRUCTURE

A. Applications of MMC topologies

As a special class of modular converters, an MMC consists of individually controllable cells. This structure provides several advantages including high scalability and reduced filter requirements while allowing for fast and independent control of instantaneous active and reactive power flow [12]. MMCs are conventionally used for bidirectional AC-DC conversion applications without any loading or generation connected at the individual modules. Modification of the MMCs such that power transfer takes place at the cell level requires changes in the cell design and the control strategy [13].

There are several studies in the literature that discuss MMC configurations with the presence of loads or generation in the individual cells. For instance, [14] investigates integration of energy storage elements in MMC cells and analyzes such a converter structure under different operating modes. Similarly, [15] studies power sources or loads in each module of MMC-based solid-state transformers. An overview on the technical considerations and emerging technologies based on MMCs for transportation electrification is presented in [16], including applications such as rail inter-ties, railway power conditioners, railway propulsion, on-board integrated chargers and battery management systems for EVs and shipboard distribution systems.

B. MMC-based EV charging topology

The reference charging topology in this work consists of an MMC with cells that supply low voltage (LV) at floating potential to wireless charging units (WCUs). The series connection of several LV cells forms an MMC arm, and each phase of the MMC topology consists of two (upper and lower) arms. An overview of the complete three-phase configuration is shown in Fig. 1. This topology enables transformer-less connection to MV distribution grids while the WCU provides galvanic isolation between the electric vehicles and the power supply. Despite the potential to save cost/volume and reduce cabling, the proposed topology requires over-sizing of the converter to cope with high circulating currents arising from unbalanced loading [10].

In this application, the loads accommodated in the cells are the EVs, which arrive in the charging facility at different times with different energy demands. Nonuniform loading in the MMC cells may lead to significant unbalance between two arms of each phase (vertical) and unbalance between the phase pairs (horizontal). Internal power flows must be controlled such that the three-phase current at the grid interface is kept balanced and sinusoidal despite the unbalanced loading. The unbalances may also lead to voltage collapse or over-voltage in the MMC cells. A control technique that guarantees the desired attributes of the current at the grid interface and equalizes the cell voltages despite unbalanced loading was presented in [10]. The unbalances between phases, arms of same phase, and cells of same arm were compensated by regulating the DC component, first and second harmonic components of the circulating current respectively. The higher unbalance requires the larger circulating currents to control the power flows with consequent larger losses during the operation. Since increased circulating currents require correspondingly increased cabling and converter sizing, which contribute to cost, weight and space coverage of the system [16], the circulating current should be kept to a minimum level.

Given the sizing of cables and equipment, the system can tolerate a certain level of unbalance. If the unbalance correction results in circulating currents exceeding the tolerable limit, the balanced grid currents and desired cell voltages can only be maintained by suspending or reducing the charging power.

III. Load allocation strategies

Load control via suspension or reduction in power supply to the EVs may result in longer stay times in the charging facility or departure with relatively smaller energy in the battery. Such circumstances may influence the satisfaction of the consumers and reduce the profits of the charging system operator significantly. The charging system operator can limit the cases that need such actions by controlling the load allocation in the MMC arms. The main contribution of this paper is an optimized strategy that minimizes the need for charging suspension/reduction by taking the future loading into account in the allocations decisions. This strategy is compared with a simple strategy that only considers current distribution of the load in the car allocation problem. Both controls determine the MMC arms to which the cars will be placed upon their arrivals.

A. Simple allocation

The simple allocation aims to equalize the number of the cars in MMC arms at a given moment without considering the future unbalances. Therefore it is formulated as a simple algorithm, (1), which loops through the MMC phases ($l \in 1,2,3$) and arms ($a \in 1,2$) and checks the number of cars in each arm at the given moment, $B_{l,a}$. The arriving car is allocated to the arm that hosts least cars.

$$l^*, a^* = \arg\min_{l,a} B_{l,a} \tag{1}$$

B. Optimized allocation

The energy demand of a car determines its charging duration in a charging station. Charging duration is the most important parameter for the allocation problem because it determines the time intervals at which unbalance will occur in the MMC. Therefore, the first step of the optimized allocation is identifying the charging duration of a car, D, by considering its battery capacity, E, and initial state of charge, SOC^0. For a given power P_C of the charger, D is then given by:

$$D = \frac{(1 - SOC^0) \cdot E}{P_C} \tag{2}$$

The calculated D is used for the identification of the charging schedule of the new car to be allocated. The charging schedule is the vector, each element $p^{new}(t)$ being the power that will be supplied to the new car at a particular time interval t within an optimization horizon T after the allocation. In effect the schedules consist of several P_C and zeros for the time intervals inside and outside of the D respectively:

$$p^{new}(t) = \begin{cases} P_C & t < D \\ 0 & t \geq D \end{cases} \tag{3}$$

The objective of the allocation problem is choosing the arm to place the new car such that the total horizontal and vertical unbalance are minimized over the considered optimization horizon. This problem can be expressed with a mixed-integer linear optimization model. The objective function, defined by (4), penalizes two time-varying dependent variables i.e. total vertical $P^{\Delta_V}(t)$ and horizontal $P^{\Delta_H}(t)$ unbalance:

$$\min_{x_{l,a}} \sum_{t=0}^{T-1} (p^{\Delta_H}(t) + p^{\Delta_V}(t)) \tag{4}$$

$P^{\Delta_V}(t)$ and $P^{\Delta_H}(t)$ are equal to the summation of absolute values of the individual arm-to-arm and phase-to-phase unbalances respectively, where $p^{\Sigma}_{l,a}(t)$ is the total power supplied by the arm (l,a) at the time interval t:

$$p^{\Delta_V}(t) = \sum_{l=1}^{3} \mid p^{\Sigma,t}_{l,1} - p^{\Sigma,t}_{l,2} \mid \tag{5}$$

$$p^{\Delta_H}(t) = \sum_{l_1 \neq l_2 \in \{1,2,3\}} \mid p^{\Sigma}_{l_1}(t) - p^{\Sigma}_{l_2}(t) \mid \tag{6}$$

The variables of the optimization problem are six binary variables, $x_{l,a} \in 0,1$, each of which represents allocation to a particular MMC arm (l,a). Summation of these binaries are always equal to one. Thus, optimization is forced to return only one result to allocate the car:

$$\sum_{l=1}^{3} \sum_{a=1}^{2} x_{l,a} = 1 \tag{7}$$

Allocation to an arm with an empty cell is ensured by a constraint, given by (8), with $B_{l,a}$ being the number of cars in the MMC arm (l,a) before the allocation. The number of cars cannot exceed the number of cells, N, after the allocation of the new car:

$$x_{l,a} + B_{l,a} \leq N \tag{8}$$

The impact of the new allocation to the system unbalance is modelled by two additional constraints. $p_{l,a,n}(t)$ is the power supplied by the n^{th} cell of the arm a of phase l at the time step t according to the charging schedule calculated in (2)-(3). The arm power $p^{\Sigma,t}_{l,a}$ is a dependent variable, which includes the power supplied to the newly assigned car $p^{new}(t)$ if it is allocated to this particular arm. With the arm powers $p^{\Sigma,t}_{l,a}$, the phase powers $p^{\Sigma,t}_{l}$ are expressed.

$$p^{\Sigma}_{l,a}(t) = p^{new}(t) \cdot x_{l,a} + \sum_{n=1}^{N} p_{l,a,n}(t) \tag{9}$$

$$p^{\Sigma}_{l}(t) = p_{l,1}(t) + p_{l,2}(t) \tag{10}$$

IV. Simulations

This section presents two tests cases. The first test shows how the decision made by the optimized allocation model differ from the decision of the simple allocation algorithm for a given initial load distribution and how these decisions lead to different future unbalances. The second part introduces a simulation scenario that includes several arrival events in a specified time window and demonstrates how simple and optimized allocation models perform in the sense of energy demand fulfillment.

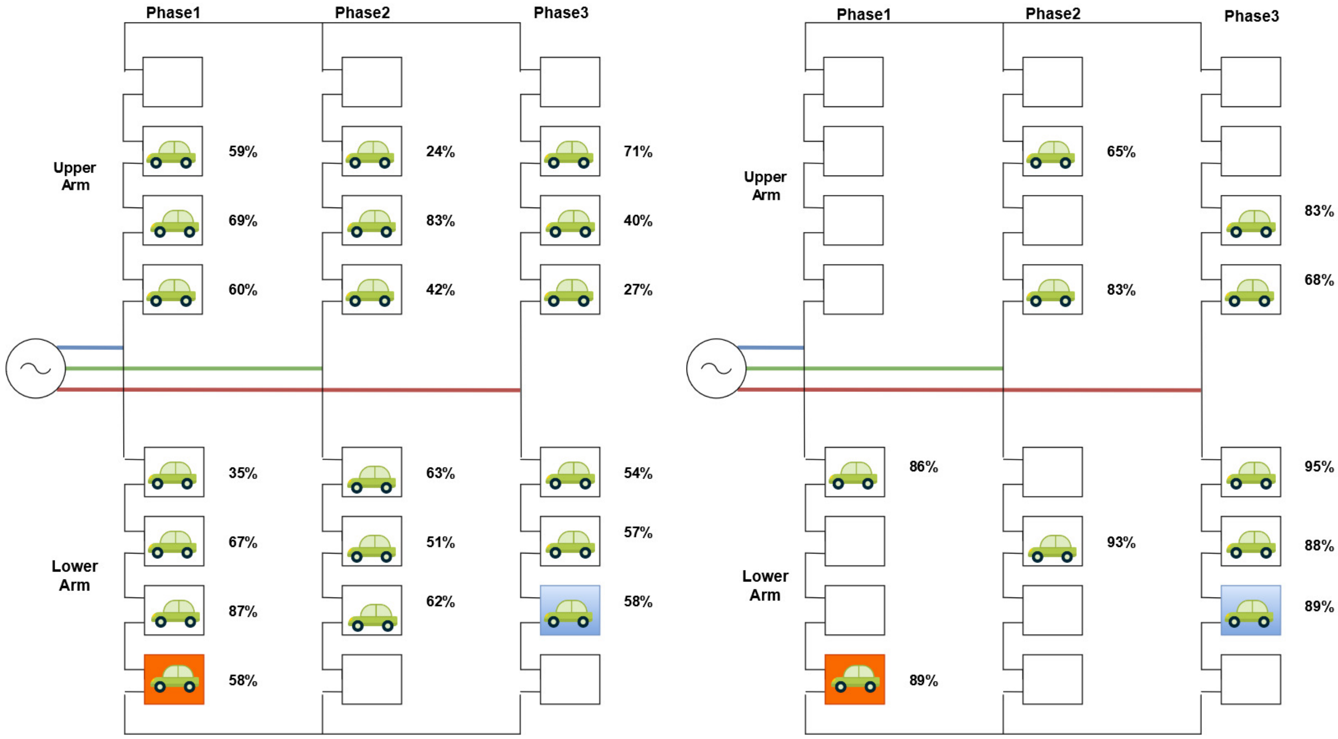

(a) Initial distribution of loads

(b) Load distribution after disconnection of charged cars

Fig. 2. Different decisions in simple vs optimized allocation

A. *Simple vs optimized allocation for given load distribution*

A simplified initial setup was considered for this test. 17 cars of the same model i.e. same battery capacity are hosted by the system. These cars stay in the car park long enough to fully charge their batteries. Their SOC at the start of the simulation range between 27-87%. Each MMC arm has 3 connected cars in their cells except for the lower arm of the phase 3, which has only 2 cars.

The two load allocation techniques were tested for the case in which another car of the same model arrives in the car park with 58% SOC. The logic of simple allocation chose the arm with minimum number of hosted cars at a given moment without considering the future unbalances and thus the car was allocated to the lower arm of the phase 3, as marked by blue in Fig. 2(a). On the other hand, a different decision was made in the optimized allocation case. The car was allocated to the lower arm of the phase 3, marked by orange in Fig. 2(a) since it causes less future unbalance.

For simplicity of the analysis, it was assumed that the energy is supplied with constant power rate, which increases the SOC of the battery by 1% in each time step. The load distribution after 41 time steps is illustrated in Fig. 2(b). In the meantime 5, 3 and 1 cars got fully charged and disconnected from phase 1, 2 and 3 respectively. The result shows that the optimal allocation reduces maximum horizontal unbalance between phase 1 and phase 3 from 4 to 2 unit power in the future. Such reductions may lead to remarkable decrease in supply interruptions in certain scenarios.

B. *Demand fulfillment by simple vs optimized allocation*

Another test was performed in order to evaluate the demand fulfillment performance of the optimized allocation model. Therefore, a test scenario was constructed, in which several cars arrive in the charging facility with the goal of charging their batteries up to 100%. For this test, a charging facility with 50 cells in each arm of the MMC i.e. a total capacity of 300 cars was considered. Each MMC cell accommodates a charging unit with $22\,\mathrm{kW}$ maximum power. It was assumed that the charging operator obtains the SOC information upon arrival and tracks it precisely during the charging. A scenario that consists of 200 arrivals was built to test the algorithms. In this scenario the cars, each having $55\,\mathrm{kWh}$ battery capacity, arrive in the charging facility with initial SOC values between 20% and 50%. Random arrival times were assigned to the cars. The departure times were selected considering their arrival times and initial SOCs such that the cars stay in the charging facility as much as the minimum time needed to charge their batteries to 100% with the given charger power. The scenario starts with the arrival of the first car at 12:00 and finishes with the departure of the last car at 15:55.

Figure 3(a) shows the unbalance that would occur in simple and optimized allocation cases if the system were sized to tolerate 100% unbalance. However, in the test scenario, the vertical and horizontal unbalances were limited with 5% of the arm and phase capacity respectively. This means that, for example, when the aggregated power of the upper arm of a phase is $55\,\mathrm{kW}$ more than the power of lower arm of the same

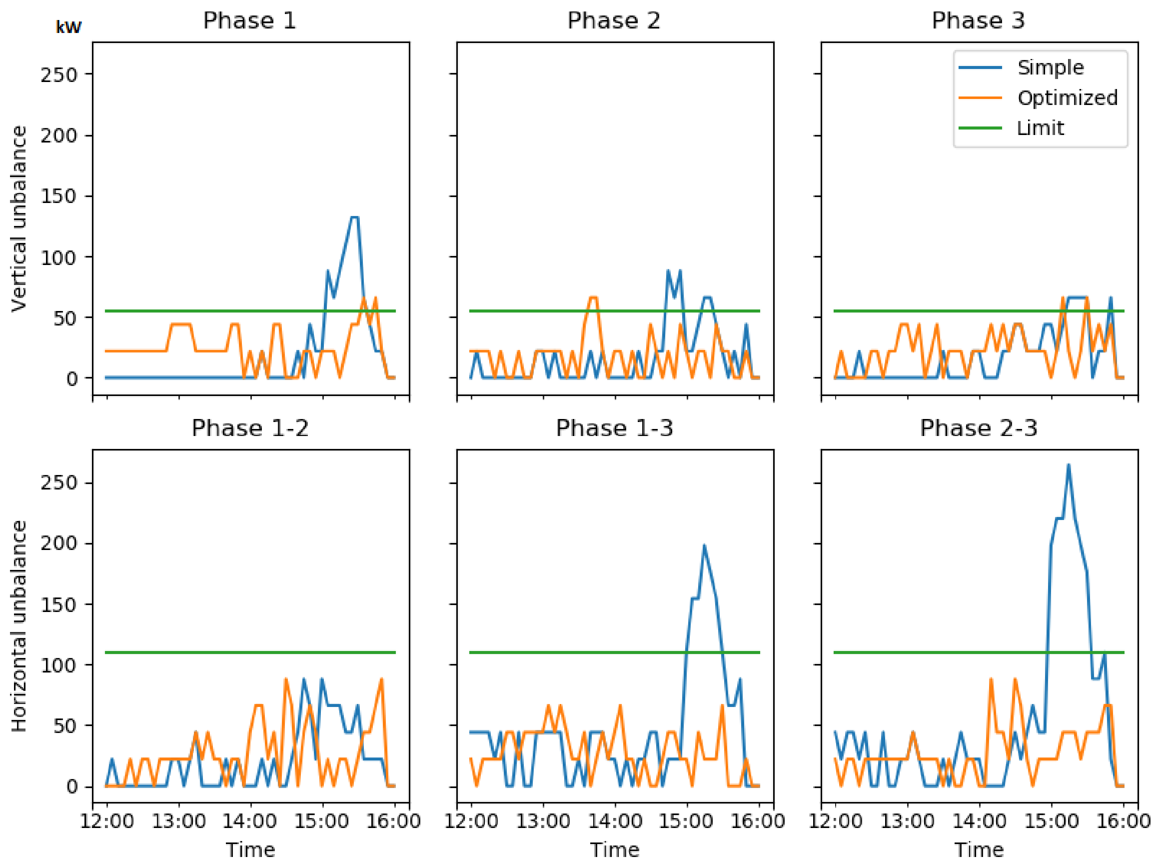

(a) Unbalance in non-constrained case

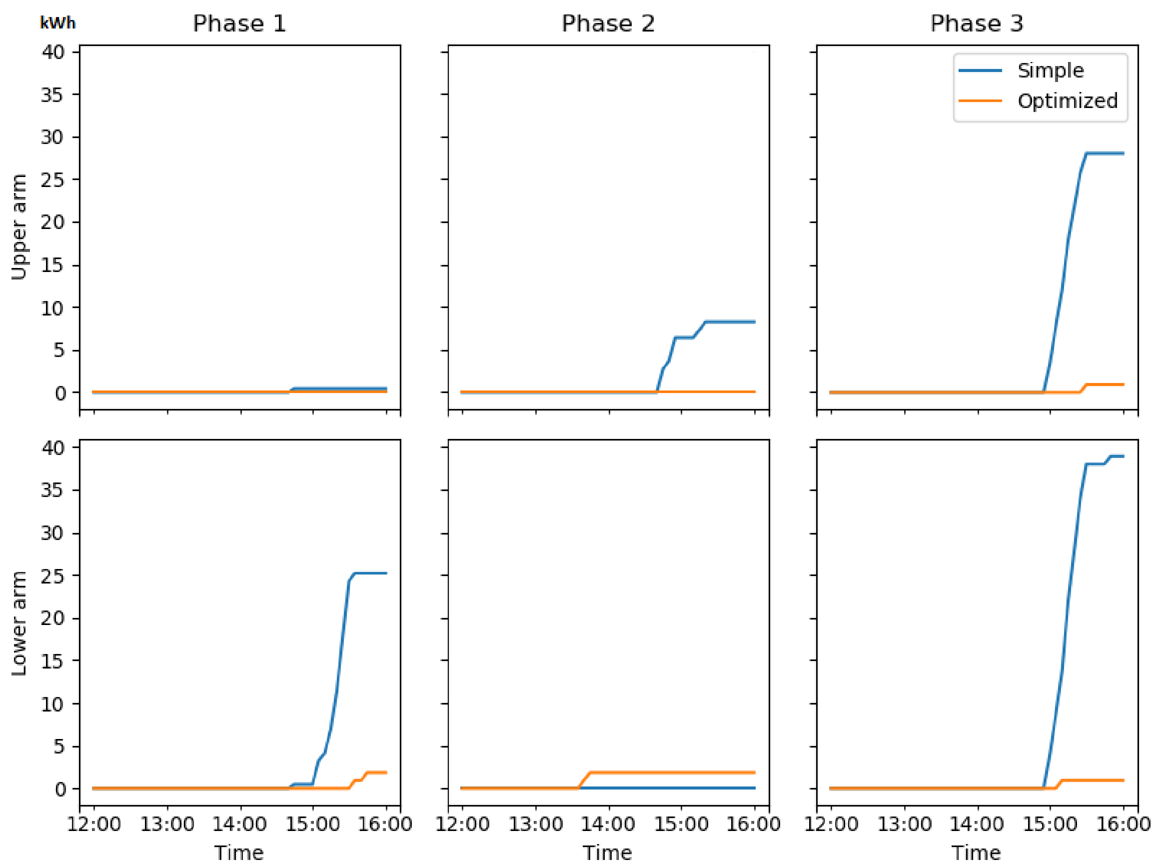

(b) Supply reduction due to unbalance

Fig. 3. Impact of optimized allocation on demand fulfillment

phase, the system works within its operational boundaries. Power supply is not suspended or reduced unless larger vertical unbalance occurs. Similarly the unbalance between two phases are not allowed to exceed $110\,\mathrm{kW}$.

The test scenario was simulated twice. The first instance simulates the scenario by implementing the simple allocation, while the second by the optimized allocation i.e. considering the future unbalances. The optimization model takes a future horizon of 4 hours with 5 minute resolution into account. In both cases a supply reduction technique was implemented, which reduces the charging power of the cells in the arms that cause the excessive unbalance. With this reduction, the unbalance is kept at the tolerable limits all the time. It should be noted that the supply reduction applies equally to each connected cells of the arm that causes excessive unbalance.

Figure 3(b) depicts the cumulative supply reduction over time in each arm for both simulated instances. Power reduction in the time intervals with extreme loading unbalance result in $101\,\mathrm{kWh}$ energy curtailment in case of simple allocation. By optimized allocation 95% of this curtailment is avoided and overall energy supply increases from $6961\,\mathrm{kWh}$ to $7056\,\mathrm{kWh}$ over two hours. Larger supply leads to increased final SOC at the end of parking duration. When the final SOCs of the identical cars were compared, it was seen that 14 out of 200 hosted cars left the charging facility with at least 5% larger final SOC in case of optimized allocation. Similarly the final SOC of 39 cars increased by at least 1%.

The results show that optimized allocation by considering the diverse individual energy demands outperforms the simple allocation model. Achieving larger final SOC increases the EV users' satisfaction from the charging service. In addition, increased capacity utilization is highly desirable for the charging system operator since larger service means earlier payback of the installation costs.

V. Conclusions

The main operational challenge in an MMC based charging topology is maintaining the correct form the 3-phase grid current and stable cell voltages despite the unbalanced distribution of the system load across the MMC arms and phases. Extreme unbalances due to the heterogeneous presence and energy demands of the EVs may require load control via suspension or reduction of the charging power. In certain scenarios this may lead to decreased user/operator satisfaction. This paper looks closely at the load allocation issue to limit the natural unbalance due to the heterogeneous presence of the loads in the MMC based system.

Two load allocation strategies were developed and tested. The results show that the strategy that allocates the EVs according to their individual energy demands would minimize the vertical and horizontal loading unbalance and thus requires less charging power reduction. The ability to limit the unbalance with proper car allocation is an important feature that may diminish the need for over-sizing the converter. Future research will be concentrated on scheduling by considering the load side flexibility in the system.

Acknowledgment

Modular Megawatt-range Wireless EV Charging Infrastructure Providing Smart Grid Services (MoMeWeC) is a research project of the international joint initiative EIG CONCERT - Japan, under the Joint Call on Efficient Energy Storage and Distribution. The authors would like to thank German Federal Ministry of Education and Research (BMBF) for providing financial support.

References

[1] J. M. Cansino, A. Sánchez-Braza, and T. Sanz-Díaz, "Policy instruments to promote electro-mobility in the EU28: A comprehensive review," *Sustainability*, vol. 10, 2018.

[2] A. Lam, S. Lee, J.-F. Mercure, Y. Cho, C.-H. Lin, H. Pollitt, U. Chewpreecha, and S. Billington, "Policies and Predictions for a Low-Carbon Transition by 2050 in Passenger Vehicles in East Asia: Based on an Analysis Using the E3ME-FTT Model," *Sustainability*, vol. 10, 2018.

[3] "Norwegian EV policy," Available at https://elbil.no/english/norwegian-ev-policy/ (2020/03/12).

[4] H. Auvinen, T. Järvi, M. Kloetzke, U. Kugler, J.-A. Bühne, F. Heinl, J. Kurte, and K. Esser, "Electromobility scenarios: research findings to inform policy," *Transportation Research Procedia*, vol. 14, pp. 2564–2573, 2016.

[5] D. F. Recalde Melo, G. Hoay Beng, and T. Massier, "Charging of electric vehicles and demand response management in a singaporean car park," in *2014 49th International Universities Power Engineering Conference (UPEC)*, 2014, pp. 1–6.

[6] M. Brenna, F. Foiadelli, M. Longo, and S. Grillo, "Charging optimization for electric vehicles in large park ride areas," in *2016 IEEE Power and Energy Society General Meeting (PESGM)*, 2016, pp. 1–5.

[7] F. Palone, M. Rebolini, S. Gentili, G. M. Giannuzzi, M. Schembari, and S. Lauria, "Connection of very large public charging station to the hv transmission grid," in *2015 IEEE 15th International Conference on Environment and Electrical Engineering (EEEIC)*, 2015, pp. 1262–1267.

[8] I. S. Bayram, G. Michailidis, and M. Devetsikiotis, "Electric power resource provisioning for large scale public EV charging facilities," in *2013 IEEE International Conference on Smart Grid Communications (SmartGridComm)*, Oct 2013, pp. 133–138.

[9] D. Strickland, T. Embley, J. Osborne, J. Yang, Z. Qiao, A. Malhotra, A. Corliss, and K. Ashworth, "Feasibility study: investigation of car park-based V2G services in the UK central hub," *The Journal of Engineering*, vol. 2019, no. 17, pp. 3967–3971, 2019.

[10] G. Guidi, S. D'Arco, J. A. Suul, R. Iso, and J. Itoh, "A modular multilevel interface for transformerless grid integration of large-scale infrastructure for wireless electric vehicle charging," in *2019 10th International Conference on Power Electronics and ECCE Asia (ICPE 2019 - ECCE Asia)*, May 2019, pp. 2059–2066.

[11] M. Mao, Y. Ding, L. Chang, N. D. Hatziargyriou, Q. Chen, T. Tao, and Y. Li, "Multi-objective power management for EV fleet with mmc-based integration into smart grid," *IEEE Transactions on Smart Grid*, vol. 10, no. 2, pp. 1428–1439, 2019.

[12] R. Marquardt, "Modular multilevel converters: State of the art and future progress," *IEEE Power Electronics Magazine*, vol. 5, no. 4, pp. 24–31, 2018.

[13] F. Briz, M. López, A. Zapico, A. Rodríguez, and D. Díaz-Reigosa, "Operation and control of mmcs using cells with power transfer capability," in *2015 IEEE Applied Power Electronics Conference and Exposition (APEC)*, 2015, pp. 980–987.

[14] M. Vasiladiotis and A. Rufer, "Analysis and control of modular multilevel converters with integrated battery energy storage," *IEEE Transactions on Power Electronics*, vol. 30, no. 1, pp. 163–175, Jan 2015.

[15] F. Briz, M. Lopez, A. Rodriguez, and M. Arias, "Modular power electronic transformers: Modular multilevel converter versus cascaded h-bridge solutions," *IEEE Industrial Electronics Magazine*, vol. 10, no. 4, pp. 6–19, Dec 2016.

[16] D. Ronanki and S. S. Williamson, "Modular multilevel converters for transportation electrification: Challenges and opportunities," *IEEE Transactions on Transportation Electrification*, vol. 4, no. 2, pp. 399–407, June 2018.